

~~CONFIDENTIAL~~

Inactive

Copy No. 8  
RM No. 18A14

OCT 31 1948

~~CONFIDENTIAL~~

CLASSIFICATION CANCELLED

NACA RM No. 18A14

Authority: NACA R 72802

~~CONFIDENTIAL~~

~~CONFIDENTIAL~~  
NACA

Date: 11/17/54

See

# RESEARCH MEMORANDUM

INVESTIGATION OF LOW-SPEED, POWER-OFF STABILITY AND CONTROL CHARACTERISTICS OF A MODEL WITH A 35° SWEEPBACK WING IN THE LANGLEY FREE-FLIGHT TUNNEL

By

Robert O. Schade

Langley Aeronautical Laboratory  
Langley Field, Va.

CLASSIFIED DOCUMENT

This document contains classified information affecting the National Defense of the United States within the meaning of the Espionage Act, USC 5031 and 32. Its transmission or the revelation of its contents in any manner to an unauthorized person is prohibited by law. Information so classified may be imparted only to persons in the military and naval services of the United States, appropriate civilian officers and employees of the Federal Government who have a legitimate interest therein, and to United States citizens of known loyalty and discretion who of necessity must be informed thereof.



NATIONAL ADVISORY COMMITTEE  
FOR AERONAUTICS

WASHINGTON  
October 28, 1948

UNCLASSIFIED

~~CONFIDENTIAL~~

NACA LIBRARY

LANGLEY MEMORIAL AERONAUTICAL  
LIBRARY  
Langley Field, Va.

~~CONFIDENTIAL~~

~~CONFIDENTIAL~~

by authority of...  
Date: 11/17/54  
Langley Aeronautical Laboratory  
Langley Field, Va.

## NATIONAL ADVISORY COMMITTEE FOR AERONAUTICS

## RESEARCH MEMORANDUM



## INVESTIGATION OF LOW-SPEED, POWER-OFF STABILITY AND CONTROL

## CHARACTERISTICS OF A MODEL WITH A 35° SWEEPBACK WING

## IN THE LANGLEY FREE-FLIGHT TUNNEL

By Robert O. Schade

## SUMMARY

An investigation has been made in the Langley free-flight tunnel to determine the low-speed, power-off dynamic stability and control characteristics of a model with a 35° sweptback wing. The investigation consisted of force and flight tests of the model and calculations of the lateral oscillatory stability with wing-tip fuel tanks off and on.

The flaps-up longitudinal stability was satisfactory except for a nosing-up tendency at the high lift coefficients, which was eliminated by use of stall-control vanes. With flaps deflected the model was longitudinally stable over the lift range, but the roll-off at the stall was more abrupt than for the flaps-retracted condition. For the configuration with tip tanks off, the lateral stability and control characteristics were generally satisfactory. With tip tanks on, however, the greatly increased moments of inertia caused an undamped rolling and yawing oscillation similar to that reported in NACA Rep. No. 769 for a model with high moments of inertia. With tip tanks on, the model was also longitudinally unstable at high lift coefficients even with stall-control vanes on because of the large rearward shift in center of gravity caused by the tanks.

## INTRODUCTION

An investigation has been made in the Langley free-flight tunnel to determine the low-speed, power-off dynamic stability and control characteristics of a model with a 35° sweptback wing. Force and flight tests of the model were made with and without stall-control vanes, trailing-edge split flaps, and wing-tip fuel tanks. Calculations were also made to determine the lateral oscillatory stability of the model with the wing-tip tanks off and on at a moderately high lift coefficient.

## SYMBOLS

W	weight, pounds
S	wing area, square feet
$i_w$	incidence of wing with respect to the fuselage water line, degrees
$\bar{c}$	mean aerodynamic chord, M.A.C., feet
l	tail length (distance from center of gravity to rudder hinge line), feet
b	wing span, feet
z	height of center of pressure of vertical tail above fuselage axis, feet
q	dynamic pressure, pounds per square foot
$\rho$	mass density of air, slugs per cubic foot
W/S	wing loading, pounds per square foot
m	mass, slugs
$\mu$	relative density factor ( $m/\rho S b$ )
$\alpha$	angle of attack of fuselage water line, degrees
$\psi$	angle of yaw, degrees
$\beta$	angle of sideslip, degrees ( $-\psi$ )
$C_L$	lift coefficient (Lift/qS)
$C_D$	drag coefficient (Drag/qS)
$C_m$	pitching-moment coefficient (Pitching moment/qS $\bar{c}$ )
$C_n$	yawing-moment coefficient (Yawing moment/qSb)
$C_l$	rolling-moment coefficient (Rolling moment/qSb)
$C_y$	lateral-force coefficient (Lateral force/qS)
$i_t$	tail incidence with respect to the fuselage water line, degrees

$\delta_e$	elevator deflection, degrees
$\delta_f$	trailing-edge-flap deflection, degrees
$-\partial C_m / \partial C_L$	static margin
$C_{Y\beta}$	rate of change of lateral-force coefficient with angle of sideslip, per degree $\left( \frac{\partial C_Y}{\partial \beta} \right)$
$C_{n\beta}$	rate of change of yawing-moment coefficient with angle of sideslip, per degree $\left( \frac{\partial C_n}{\partial \beta} \right)$
$C_{l\beta}$	rate of change of rolling-moment coefficient with angle of sideslip, per degree $\left( \frac{\partial C_l}{\partial \beta} \right)$
$C_{l_p}$	rate of change of rolling-moment coefficient with rolling-angular-velocity factor $\left( \frac{\partial C_l}{\partial \frac{pb}{2V}} \right)$
$C_{n_p}$	rate of change of yawing-moment coefficient with rolling-angular-velocity factor $\left( \frac{\partial C_n}{\partial \frac{pb}{2V}} \right)$
$C_{l_r}$	rate of change of rolling-moment coefficient with yawing-angular-velocity factor $\left( \frac{\partial C_l}{\partial \frac{rb}{2V}} \right)$
$C_{n_r}$	rate of change of yawing-moment coefficient with yawing-angular-velocity factor $\left( \frac{\partial C_n}{\partial \frac{rb}{2V}} \right)$
$k_X$	radius of gyration about longitudinal body axis, feet
$k_Z$	radius of gyration about vertical body axis, feet
$k_{XZ}$	product-of-inertia factor about body axis, feet <sup>2</sup>
$\gamma$	flight-path angle, degrees

- $\epsilon$  angle between body axis and principal axis, positive when reference axis is above principal axis, at the nose of the airplane, degrees
- $\eta$  angle of attack of principal longitudinal axis of airplane, positive when principal axis is above flight path, degrees ( $\alpha - \epsilon$ )
- R Routh's discriminant

#### APPARATUS

##### Wind Tunnel

The tests were made in the Langley free-flight tunnel, which is designed to test free-flying dynamic models. A complete description of the tunnel and its operation is given in reference 1.

Force tests to determine the static stability characteristics of the model were conducted with the Langley free-flight-tunnel six-component balance described in reference 2. This balance rotates with the model in yaw so that all forces and moments are measured with respect to the stability axes. The stability axes are shown in figure 1.

##### Model

A three-view drawing of the model is presented in figure 2, and photographs of the model are given as figures 3 and 4. Table I gives the dimensional and mass characteristics of the model.

The wing of the model had a Rhode St. Genese 35 airfoil section. The use of this section was in accordance with free-flight-tunnel practice of using airfoils to obtain a maximum lift coefficient in low-scale tests more nearly equal to that of a full-scale design. The wing was set at  $-6^\circ$  incidence with respect to the fuselage so that zero lift would be obtained at approximately zero angle of attack of the fuselage.

Stall-control vanes, trailing-edge split flaps, and wing-tip tanks were installed for some tests. The intake ducts were faired (fig. 2) after the initial tests had shown that severe air-flow separation at the wing-fuselage juncture was caused by the flat surface of the duct opening. (See fig. 4.)

## TESTS

## Force Tests

The force tests were run at a dynamic pressure of 3.0 pounds per square foot which corresponds to an airspeed of approximately 34 miles per hour at standard sea-level conditions and to a test Reynolds number of 282,000 based on the mean aerodynamic chord of 0.884 foot. All but the initial tests were made with the intake-duct fairings on. A summary of the force-test conditions is given in table II.

All forces and moments are referred to the stability axes originating at a center-of-gravity position of 22.0 percent of the mean aerodynamic chord and located vertically 26.0 percent of the mean aerodynamic chord above the bottom of the fuselage (water line zero) unless otherwise indicated.

## Flight Tests

Flight tests were made to determine the general flying characteristics of the model. A summary of the test conditions is given in table III. Flights were made with vanes on and off, flaps up and down, and tip tanks on and off. With the tip tanks off, most of the flights were made with a light wing loading (see table I), but a few flights were made with a heavier wing loading to determine the effect of mass on the stability and control characteristics. The tip-tanks-on flights were made with the tip tanks fully loaded and the model in the light condition. All flights were made with a center-of-gravity location of 22.0 percent mean aerodynamic chord.

## CALCULATIONS

Boundaries for neutral-lateral-oscillatory stability ( $R = 0$ ) were calculated for the model with tip tanks off and on by means of the stability equations of reference 3 and are shown in figure 5 as functions of  $C_{n\beta}$  and  $-C_{l\beta}$ . With the tanks off the calculations were made for the heavy condition. With the tanks on the calculations were made for the only tank-on condition flown.

The values of the static-lateral-stability derivatives  $C_{Y\beta}$ <sub>tail-off</sub> and  $C_{n\beta}$ <sub>tail-off</sub> were estimated from force tests; the rotary derivatives  $C_{n_r}$  and  $C_{l_r}$  were estimated from unpublished data; and values of  $C_{l_p}$  and  $C_{n_p}$  were obtained from rotation tests of the model. The values

of  $k_x$  and  $k_z$  and the inclination of principal axes of inertia were measured for the model. The values of all the aerodynamic and mass characteristics used in the calculations are given in table IV.

The values of  $C_{n\beta}$  and  $-C_{l\beta}$  for the model with tip tanks off and on at  $C_L = 0.7$ , as determined from force tests, are indicated by symbols in figure 5 in order to show their relation to the calculated stability boundaries.

## RESULTS AND DISCUSSION

### Force Tests

The results of the force tests made to determine the static longitudinal and lateral stability characteristics are presented in figures 6 to 13. Unpublished data from larger scale tests ( $R = 2,243,000$ ) of a larger model at UWAL (University of Washington Aeronautical Laboratory) are also presented for comparison. The UWAL data were obtained at a dynamic pressure of 30.21 pounds per square foot and the pitching moments were referred to a center of gravity at 20.0 percent of the mean aerodynamic chord.

The results presented in figures 6(a) and 6(b) show the longitudinal stability characteristics of the free-flight-tunnel model with and without the intake-duct fairing. Also presented for comparison are the UWAL results which were obtained with the intake ducts open. Preliminary tuft surveys had indicated the need for fairing the closed intake ducts on the free-flight-tunnel model, since severe air-flow separation was noted behind the ducts. It is seen from figure 6(a) that the complete model became unstable above  $C_L = 0.75$  without the fairing, and the addition of the fairing not only delayed the instability to  $C_L = 0.85$  but greatly reduced its severity. The fairing also reduced the static margin  $-\partial C_m / \partial C_L$  by about 0.05 over the lower lift range. The results of the UWAL tests show fairly good agreement with the free-flight-tunnel tests without the fairing, which might be an indication that the flow in the region of the ducts of the UWAL model must also have been unsatisfactory. It appears that attention must be given to obtaining the best possible flow through and around the ducts since this flow apparently has a pronounced effect on the stability. The data of figure 6(b) show that the fairing had little effect on the tail-off longitudinal stability. This indicates that the improvement in stability of the model with tail on, produced by the addition of the fairing, was caused by a change in the nature of the flow at the tail and not by any appreciable change in stability of the wing-fuselage combination.

The data of figure 7 show the effect of the stall-control vanes for both models. The use of the vanes improved the stability of the free-flight-tunnel model, but there was still slight instability at lift

coefficients from 0.8 to 0.9. The UWAL model with vanes on was stable over the entire lift range, which indicates that a similar airplane would probably have satisfactory static longitudinal stability for this condition.

Figure 8 shows the effect of flap deflection on the longitudinal stability of the model with vanes on. It is seen that the flap resulted in the model being stable over the entire lift range except for a very slight instability at the stall. The flap also resulted in the lift curve being more nearly linear up to the maximum lift coefficient.

The variation of the lateral-stability parameters  $C_{Y\beta}$ ,  $C_{n\beta}$ , and  $C_{l\beta}$  with lift coefficient with flaps retracted is shown in figure 9 together with UWAL results with intake ducts open. It may be seen that the fairing had little effect on the directional-stability parameter  $C_{n\beta}$ . Fairly good agreement with UWAL directional-stability data was obtained for the lift-coefficient range above  $C_L = 0.48$ . The directional stability of the free-flight-tunnel model decreased gradually with increasing lift coefficient and then dropped sharply at the stall. This effect could not be verified by the UWAL results because data were unavailable for lift coefficients above 0.8. The fairing reduced the effective dihedral  $-C_{l\beta}$  over the lift range with the greatest reduction taking place at the high lift coefficients. Tuft tests indicated that the difference could be accounted for by the fact that the fairing delayed the stall on the trailing wing. The UWAL data show less effective dihedral than the free-flight-tunnel model over the lift range.

Data showing the effect of the stall-control vanes on the lateral stability characteristics are presented in figure 10. The vanes reduced both the directional stability and effective dihedral over the entire lift range.

Figure 11 shows the effect of flap deflection on the lateral stability characteristics. Deflecting the flaps eliminated the gradual decrease in directional stability with increasing lift coefficient, but the sharp drop in stability at the stall remained. The variation of the effective dihedral with lift coefficient for the flap-retracted condition was extended linearly from  $C_L = 0.85$  to  $C_L = 1.24$  when the flaps were deflected, and this resulted in an increase in the maximum value of  $-C_{l\beta}$  of about 0.001 over the flap-up condition.

The data of figure 12 show the effect of the wing-tip tanks and the center-of-gravity position on the longitudinal stability characteristics of the free-flight-tunnel model. The tip tanks had very little aerodynamic effect on the stability as shown by the data presented about the tank-off center-of-gravity location of 0.22 mean aerodynamic chord.

The model with tip tanks on was unstable at high lift coefficients, however, for the tank-on center-of-gravity location of 0.35 mean aerodynamic chord.

Figure 13 shows the comparison of the lateral stability characteristics with and without the wing-tip tanks. The tanks had little effect on the directional stability at low lift coefficients but delayed the decrease in directional stability to a higher lift coefficient. Addition of the wing-tip tanks increased the effective dihedral over most of the lift range.

#### Flight Tests

Flaps retracted. - Flight tests made over a lift-coefficient range of 0.48 to 1.0 with the model in the light-loading condition with tip tanks off showed that the lateral stability characteristics were satisfactory with stall-control vanes off or on, despite the decrease of  $C_{n\beta}$  at the high lift coefficients as indicated by the force-test results (fig. 10). The behavior of the model was good with coordinated ailerons and rudder or with ailerons alone, and the lateral oscillations were well damped.

Without the stall-control vanes the longitudinal stability of the model was good at the lower lift coefficients. At the higher lift coefficients (above 0.75), however, the model exhibited a nosing-up tendency, which can be explained by the pitching-moment curve in figure 7, and tried continually to trim at a higher angle of attack. The nosing-up motion was fairly gentle and the model could usually be controlled satisfactorily with the elevator, but for flights at the highest lift coefficients the nosing-up tendency sometimes resulted in the model stalling and rolling off on either wing. The roll-off was not particularly violent; but since there was almost complete loss of lateral control, the model usually crashed into the tunnel wall out of control.

One interesting point observed during these tests was the ability of the pilot to sometimes retain control of the model after it had started to stall by nosing it down with the elevator and thereby unstalling the wing. In tests of some tailless models with similar nosing-up tendencies but with ineffective elevators at the stall, it has been impossible to control the models once they started to stall. In the case of this model, however, the elevator on the horizontal tail remained effective and enabled the pilot to maintain a certain amount of control over the nosing-up motion.

Flights made over approximately the same speed range with the stall-control vanes on (fig. 7) showed that the vanes improved the longitudinal flight behavior of the model at high lift coefficients but still did not make the model entirely satisfactory. At the high lift coefficients, the model would trim at a new angle of attack when disturbed by elevator control or a gust, indicating about neutral stability, but it did not have

the definite nosing-up tendency exhibited with the vanes off. Since the UWAL force-test results indicated static longitudinal stability over the entire lift range with the vanes on and because the full-scale Reynolds number would be even larger than that of the UWAL tests, a similar airplane would probably be completely satisfactory in this respect if stall-control vanes are used. When the stall was reached, the model settled to the tunnel floor with aileron control being maintained at all times so that the wings could be kept level.

Flaps extended.- With flaps deflected (stall-control vanes on) the longitudinal and lateral stability characteristics of the model were good over the entire lift-coefficient range (0.51 to 1.15). There was no nosing-up tendency and all oscillations were well damped. At the stall the model rolled rather abruptly to a medium angle of bank and slid off into the tunnel wall. When ailerons alone were used for lateral control, the model flew about as well as with coordinated aileron and rudder and there was no noticeable adverse yawing.

Increased wing loading.- Increasing the wing loading of the model with tip tanks off resulted in no noticeable change in the flight behavior of the model over the lift-coefficient range flown (0.6 to 0.75 with flaps retracted and 0.85 to 0.95 with flaps deflected). At  $C_L = 0.75$  with flaps retracted there appeared to be a slight nosing-up tendency as in the lightly loaded condition at about the same lift coefficient. Good flights were obtained with either ailerons and rudder or ailerons alone used for lateral control. Results of the calculations presented in figure 5 show that the location of the model test point was on the stable side of its oscillatory-stability boundary.

Wing tanks on.- The results of flight tests made at  $C_L = 0.66$  with the wing-tip tanks on (flaps retracted) indicated a dangerous condition with coordinated aileron and rudder control. There was a lightly damped rolling and yawing motion and the model was very slow in returning from a yawed position because of the high value of  $I_z$ . At times the swinging motion appeared to be reinforced by control deflections, and flights in this condition often ended with the model crashing into the tunnel wall. It was found that the model was much easier to fly when ailerons alone were used for lateral control. There were still large yawing motions, however, and the model would sometimes stay in a yawed attitude and slip off into a wall. The poor flying characteristics were caused mainly by the large increase in inertia forces which resulted in the calculated oscillatory-stability boundary moving up so that the test point then fell in the unstable region on the chart. (See fig. 5.) This effect of mass distribution on lateral stability is in agreement with the results of reference 4, which showed that as weight was added at the wing tips the lateral stability became progressively worse.

The longitudinal stability of the model was satisfactory with the center-of-gravity location of 0.22 mean aerodynamic chord. No flights were attempted with the design center-of-gravity location of 0.35 mean aerodynamic chord since force-test results (fig. 13) indicated that the model was statically longitudinally unstable above  $C_L = 0.75$ .

A change in tank configuration, such as the use of a belly tank or an inboard shift of the wing tanks, would result in improved longitudinal and lateral stability characteristics by reducing the rearward shift of the center of gravity as well as the values of  $I_x$  and  $I_z$ .

### CONCLUSIONS

The following conclusions were drawn from the results of the free-flight-tunnel stability and control investigation of a model with a  $35^\circ$  sweptback wing.

1. With flaps retracted and no stall-control vanes, the model had satisfactory longitudinal stability up to  $C_L = 0.75$ . At higher lift coefficients, however, the model had a nosing-up tendency which sometimes caused it to stall and roll off out of control.

2. Use of stall-control vanes improved the longitudinal stability and lateral control at high lift coefficients but did not make the model entirely satisfactory. Higher scale force-test data, however, indicate that a similar full-scale airplane would probably have satisfactory longitudinal stability at the high lift coefficients if stall-control vanes were used.

3. With flaps deflected the model was longitudinally stable over the lift range, but the roll-off at the stall was more abrupt than for the flap-retracted condition.

4. The lateral stability and control characteristics were considered to be generally satisfactory for all conditions tested without the tip tanks, and the rolling and yawing motions were well damped.

5. With tip tanks on, the greatly increased moments of inertia caused an undamped rolling and yawing oscillation similar to that reported in NACA Rep. No. 769 for a model with high moments of inertia. With tip tanks on, the model was also longitudinally unstable at high lift coefficients even with stall-control vanes on because of the large rearward shift in center of gravity caused by the tanks.

Langley Aeronautical Laboratory  
National Advisory Committee for Aeronautics  
Langley Field, Va.

## REFERENCES

1. Shortal, Joseph A., and Osterhout, Clayton J.: Preliminary Stability and Control Tests in the NACA Free-Flight Wind Tunnel and Correlation with Full-Scale Flight Tests. NACA TN No. 810, 1941.
2. Shortal, Joseph A., and Draper, John W.: Free-Flight-Tunnel Investigation of the Effect of the Fuselage Length and the Aspect Ratio and Size of the Vertical Tail on Lateral Stability and Control. NACA ARR No. 3D17, 1943.
3. Sternfield, Leonard: Effect of Product of Inertia on Lateral Stability. NACA TN No. 1193, 1947.
4. Campbell, John P., and Seacord, Charles L., Jr.: The Effect of Mass Distribution on the Lateral Stability and Control Characteristics of an Airplane as Determined by Tests of a Model in the Free-Flight Tunnel. NACA Rep. No. 769, 1943.

TABLE I. - DIMENSIONAL AND MASS CHARACTERISTICS OF THE MODEL  
 WITH A 35° SWEEPBACK WING TESTED IN THE  
 LANGLEY FREE-FLIGHT TUNNEL

	Light	Heavy
Weight, lb		
Without tip tanks . . . . .	7.74	16.57
With tip tanks . . . . .		15.70
Relative density factor (m/ρSb)		
Without tip tanks . . . . .	7.26	15.56
With tip tanks . . . . .		14.75
Center-of-gravity location, percent M.A.C.		
Without tip tanks . . . . .		22
With tip tanks		
Design location based on tank weight and position . . . . .		35
Used in flight tests . . . . .		22
Distance above bottom of fuselage, percent M.A.C. . . . .		26
Moments of inertia, without tip tanks		
I <sub>X</sub> , slug-ft <sup>2</sup> . . . . .	0.122	0.122
I <sub>Z</sub> , slug-ft <sup>2</sup> . . . . .	0.581	0.581
I <sub>Y</sub> , slug-ft <sup>2</sup> . . . . .	0.478	0.478
Moments of inertia, with tip tanks		
I <sub>X</sub> , slug-ft <sup>2</sup> . . . . .		0.701
I <sub>Z</sub> , slug-ft <sup>2</sup> . . . . .		1.215
I <sub>Y</sub> , slug-ft <sup>2</sup> . . . . .		0.532
Wing loading, W/S, lb/sq ft		
Without tip tanks . . . . .	2.11	4.73
With tip tanks . . . . .		4.49
Wing		
Area, sq ft . . . . .		3.50
Span, ft . . . . .		3.97
Sweepback, c/4, deg . . . . .		35
Incidence, deg . . . . .		-6.0
Dihedral, deg (mean line) . . . . .		-1.5
Taper ratio . . . . .		0.29
Aspect ratio . . . . .		4.5
M.A.C., ft . . . . .		0.976

TABLE I.- DIMENSIONAL AND MASS CHARACTERISTICS - Concluded

	Light	Heavy
Location of leading edge M.A.C. behind leading edge of root chord, ft . . . . .	0.683	
Root chord, ft . . . . .	1.375	
Tip chord, ft . . . . .	0.392	
Distance from nose to leading edge of root chord, ft . . . . .	1.292	
Aileron		
Area, percent wing area, (one) . . . . .	2.64	
Span, percent wing span, (one) . . . . .	27.8	
Hinge location, percent chord . . . . .	75	
Vertical tail		
Area, sq ft . . . . .	0.460	
Span, ft . . . . .	0.80	
Aspect ratio . . . . .	1.39	
Sweepback, c/4, deg . . . . .	35	
Horizontal tail		
Area, sq ft . . . . .	0.67	
Span, ft . . . . .	1.53	
Aspect ratio . . . . .	3.5	
Sweepback, c/4, deg . . . . .	35	



TABLE II

## SUMMARY OF FORCE-TEST CONDITIONS

Test	Configuration					$\alpha$ (deg)	$\psi$ (deg)	Figure
	Type of Test	Fairing	Vanes	Flaps	Tanks			
1	Longitudinal	Off and on	Off	Up	Off	0-22	0	6
2	Longitudinal	On	Off and on	Up	Off	0-22	0	7
3	Longitudinal	On	On	0° and 50°	Off	0-22	0	8
4	Lateral	Off and on	Off	Up	Off	0-22	-5 and 5	9
5	Lateral	On	Off and on	Up	Off	0-22	-5 and 5	10
6	Lateral	On	On	0° and 50°	Off	0-22	-5 and 5	11
7	Longitudinal	On	On	Up	Off and on	0-22	0	12
8	Lateral	On	On	Up	Off and on	0-22	-5 and 5	13



TABLE III

## SUMMARY OF FLIGHT-TEST CONDITIONS

[All tests made at a center-of-gravity location of 21.9 percent M.A.C.]

Test	Configuration				$C_L$ range	Weight (lb)
	Vanes	Flaps	Tanks	Loading		
1	Off	0°	Off	Light	0.48 to 1.0	7.51
2	On	0°	Off	Light	0.48 to 1.0	7.51
3	On	50°	Off	Light	0.51 to 1.15	7.96
4	On	0°	Off	Heavy	0.60 to 0.75	16.49
5	On	50°	Off	Heavy	0.66 to 0.69	16.49
6	On	0°	On	Tip tanks fully loaded, model in light condition	0.66	15.69



TABLE IV.- CHARACTERISTICS OF THE MODEL USED IN THE CALCULATIONS

	Condition I tip tanks off	Condition II tip tanks on
W, lb	16.5	15.7
W/S	4.73	4.49
b, feet	3.97	3.97
$\rho$	0.00238	0.00238
$\mu$	15.56	14.7
$k_{YB}$	.459	1.199
$k_{ZB}$	.908	1.616
$k_{XZ}$	-.0541	-.1032
l/b	.643	.643
z/b	.162	.162
$C_L$	.70	.70
$\alpha$ , deg	12.0	12.0
$\epsilon$ , deg	5	5
$\eta$ , deg	7	7
$\gamma$ , deg	-10.0	-10.0
$C_{Y\beta}$	$-.115 + C_{Y\beta}(\text{tail})$	$-.115 + C_{Y\beta}(\text{tail})$
$^a C_{n\beta}$	$-.012 + C_{n\beta}(\text{tail})$	$-.012 + C_{n\beta}(\text{tail})$
$^a C_{l_p}$	$-.30 + C_{l_p}(\text{tail})$	$-.30 + C_{l_p}(\text{tail})$
$^a C_{n_p}$	$-.1242 + C_{n_p}(\text{tail})$	$-.1242 + C_{n_p}(\text{tail})$
$^a C_{l_r}$	$.175 + C_{l_r}(\text{tail})$	$.175 + C_{l_r}(\text{tail})$
$^a C_{n_r}$	$-.006 + C_{n_r}(\text{tail})$	$-.006 + C_{n_r}(\text{tail})$
$C_{Y\beta}(\text{tail})$	variable	variable
$C_{l\beta}$	Dependent variable	Dependent variable

<sup>a</sup>Tail contributions are determined from the following equations:



$$C_{n\beta}(\text{tail}) = -\frac{l}{b} C_{Y\beta}(\text{tail})$$

$$C_{l_p}(\text{tail}) = 2 \left( \frac{z}{b} - \frac{l}{b} \sin \alpha \right)^2 C_{Y\beta}(\text{tail})$$

$$C_{n_p}(\text{tail}) = C_{l_r}(\text{tail}) = -2 \frac{l}{b} \left( \frac{z}{b} - \frac{l}{b} \sin \alpha \right) C_{Y\beta}(\text{tail})$$

$$C_{n_r}(\text{tail}) = 2 \left( \frac{l}{b} \right)^2 C_{Y\beta}(\text{tail})$$

<sup>b</sup>Varied systematically as independent variable to provide the desired range of  $C_{n\beta}$  for the determination of the oscillatory stability boundary.

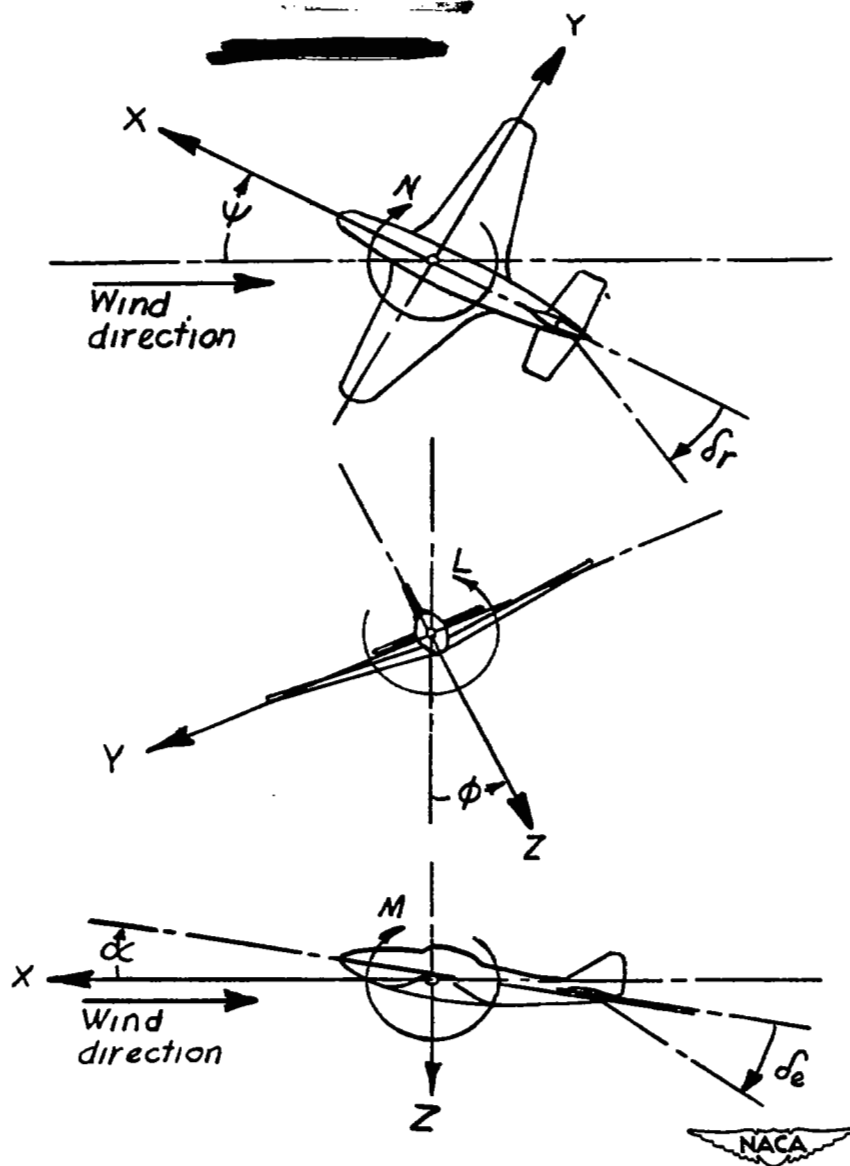


Figure 1.- The stability system of axes. Arrows indicate positive directions of moments, forces, and control-surface deflections. This system of axes is defined as an orthogonal system having their origin at the center of gravity and in which the Z-axis is in the plane of symmetry and perpendicular to the relative wind, the X-axis is in the plane of symmetry and perpendicular to the Z-axis, and the Y-axis is perpendicular to the plane of symmetry.

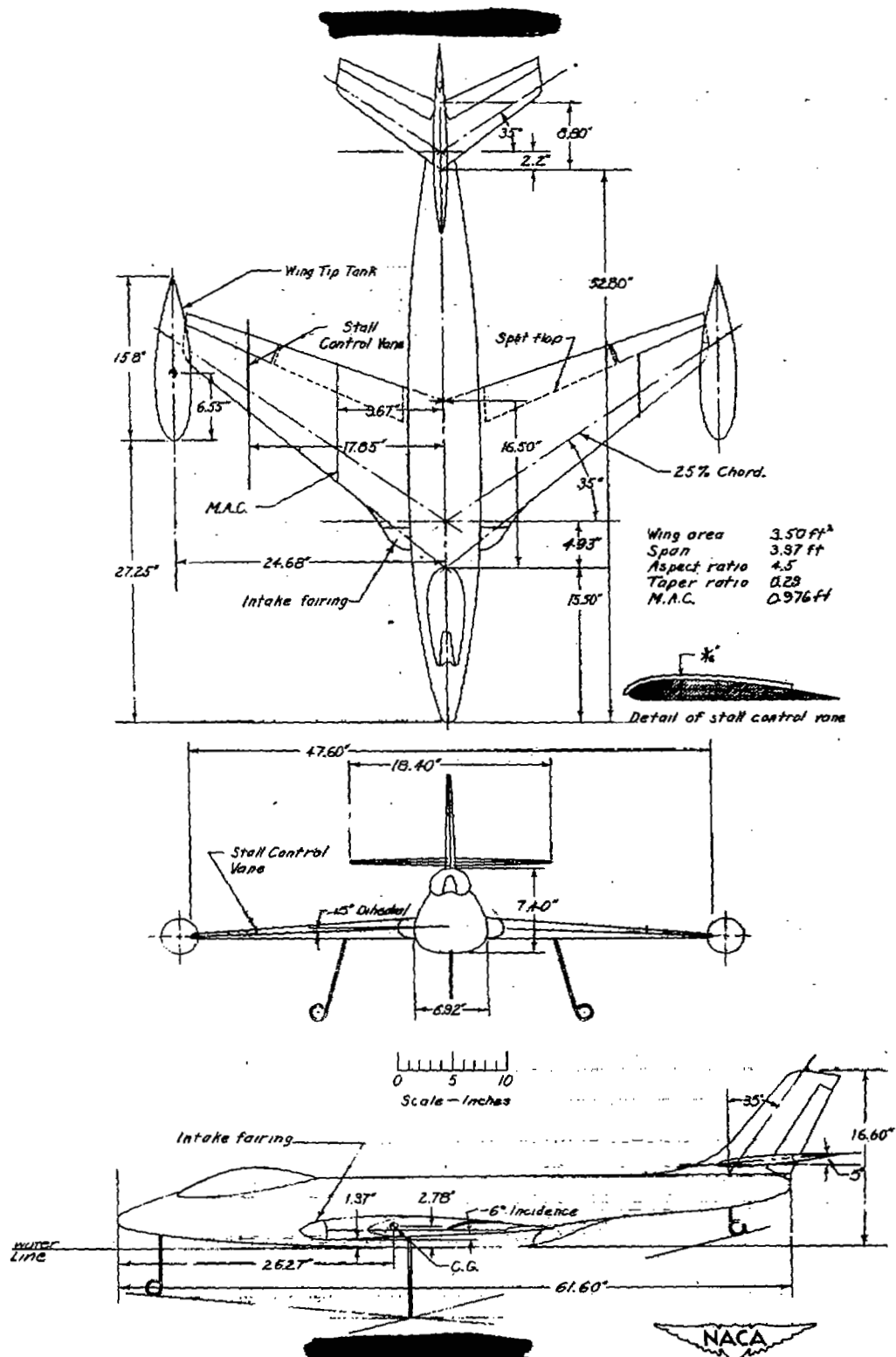


Figure 2.- Three-view drawing of the model with a 35° sweptback wing tested in the Langley free-flight tunnel.

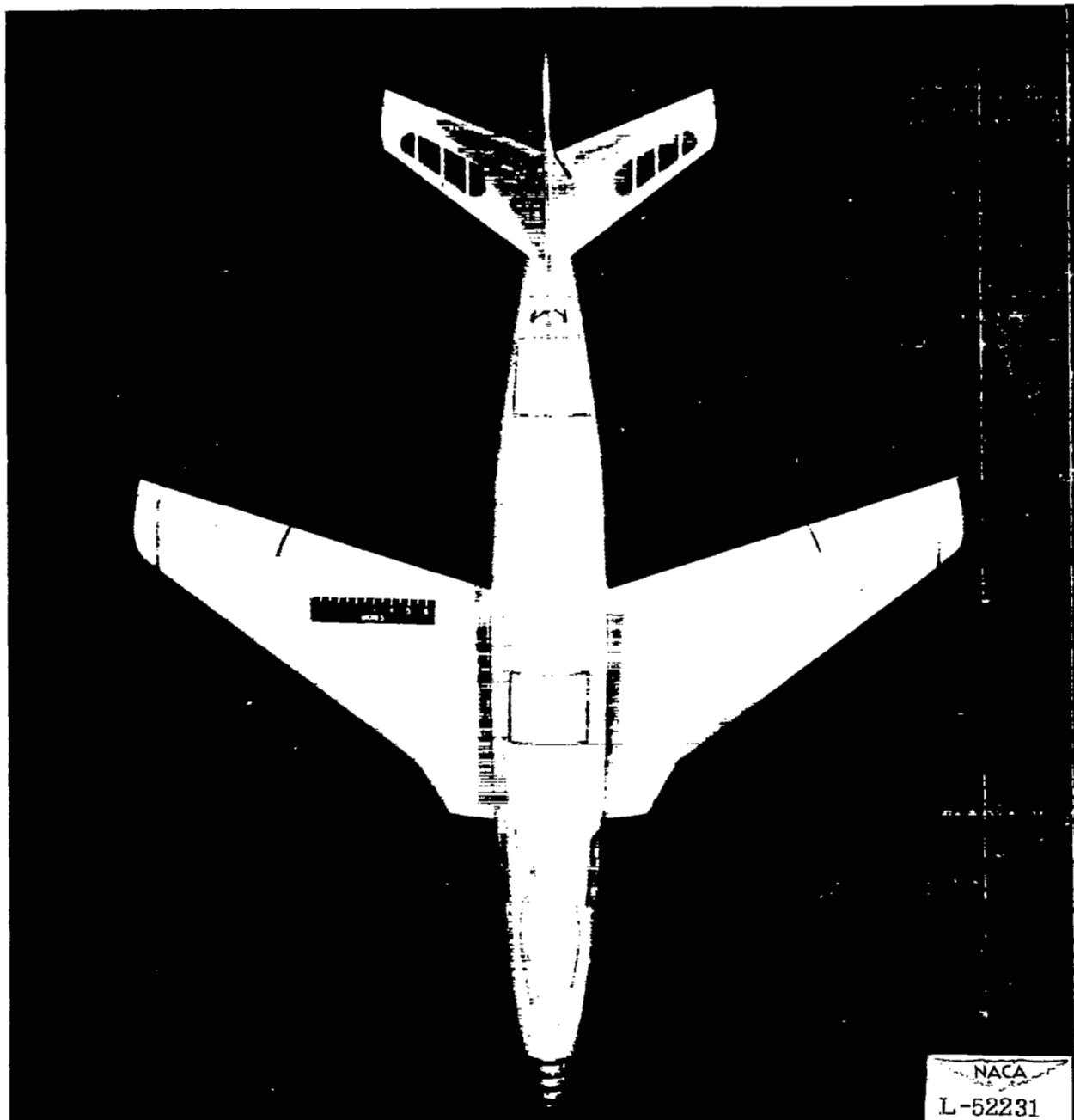


Figure 3.- Plan view of model with a  $35^{\circ}$  sweptback wing. Intake-duct fairings off.



.

.

.

.

.

.

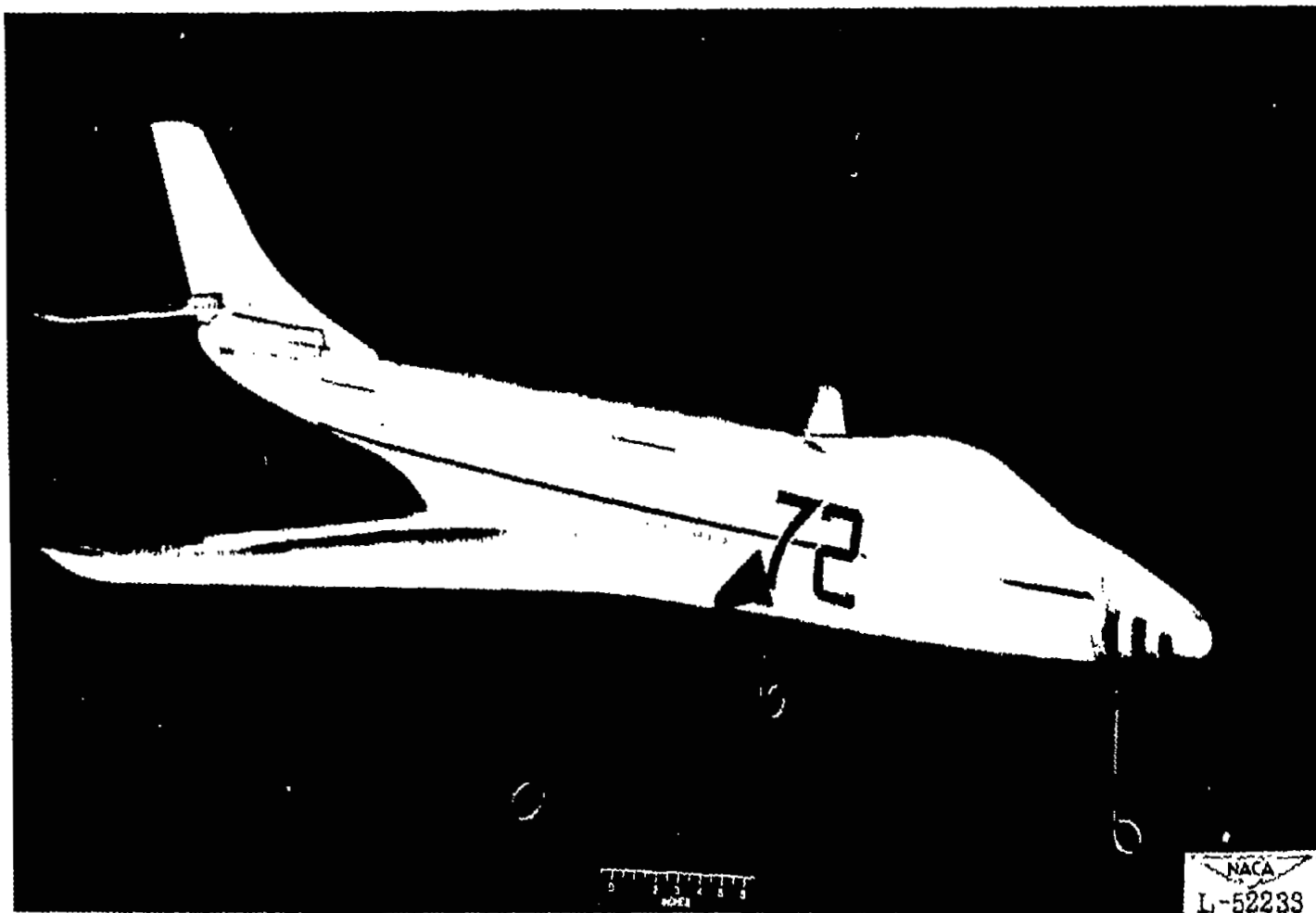


Figure 4.- Three-quarter front view of model with a  $35^\circ$  sweptback wing. Intake-duct fairings off.





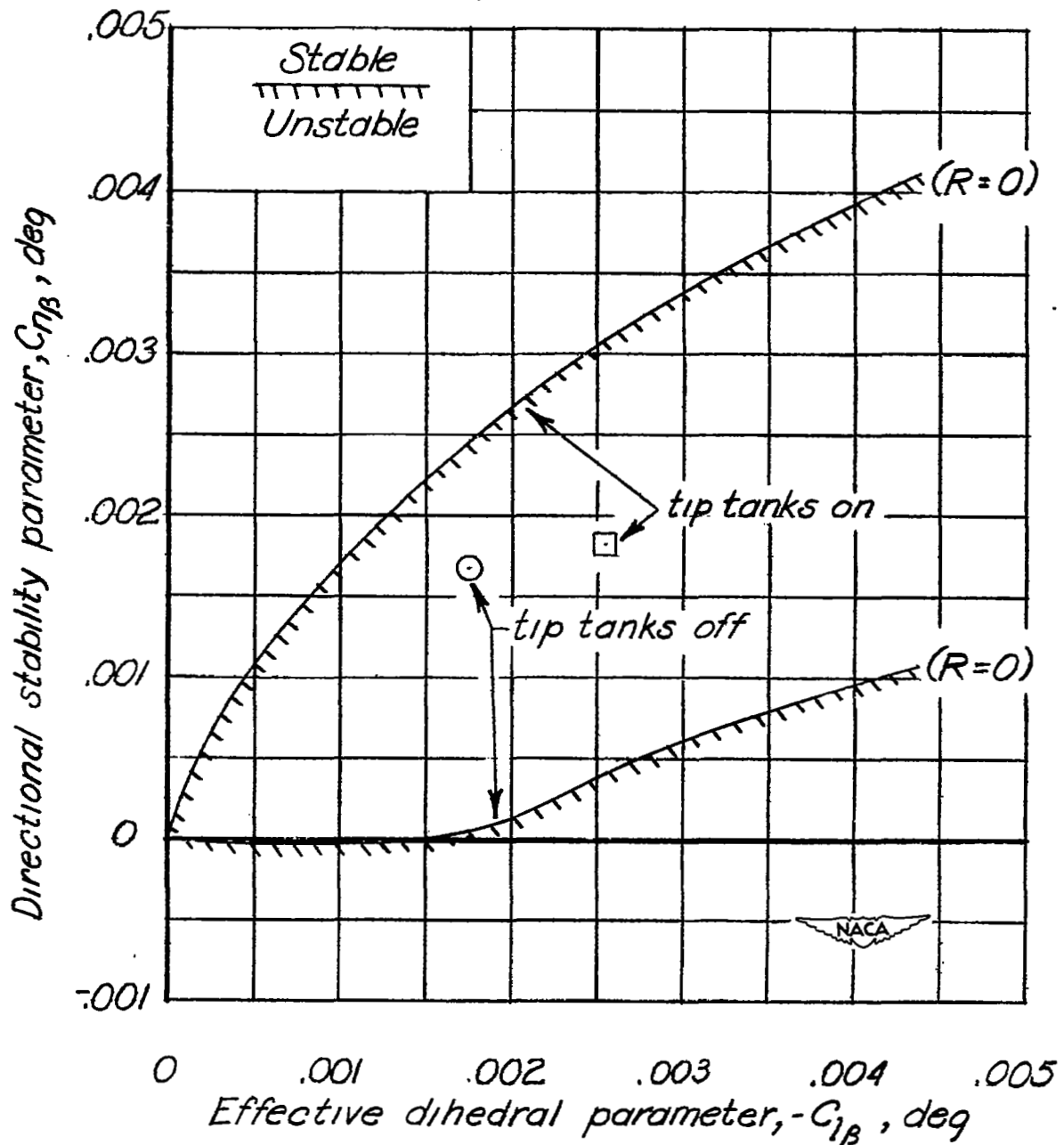
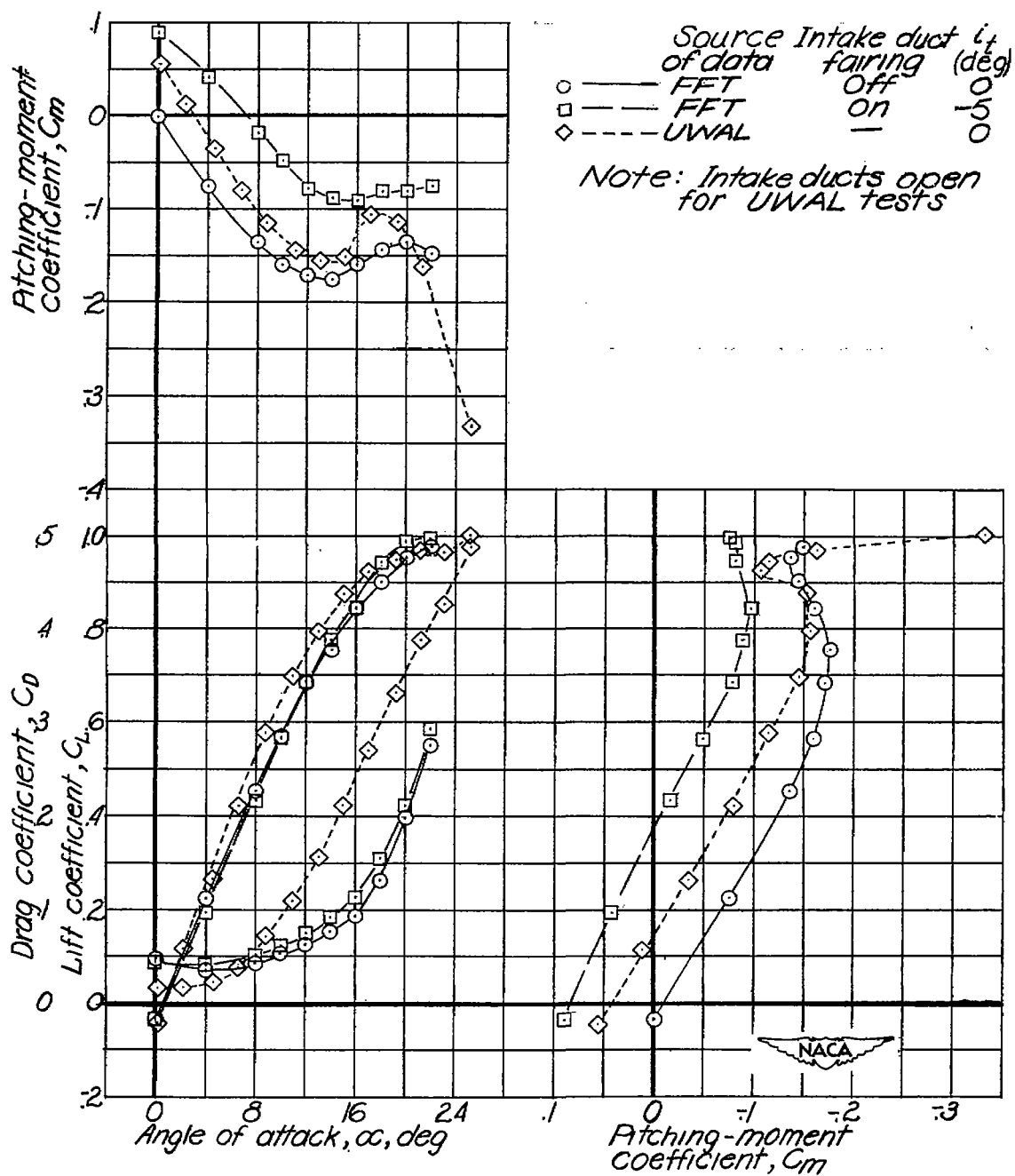


Figure 5.- Correlation of flight test points of a model with a  $35^\circ$  sweptback wing with calculated oscillatory stability boundaries;  $C_L = 0.7$ ;  $\delta_f = 0^\circ$ ; vanes and intake-duct fairings on.



(a) Tail on.

Figure 6.- Effect of intake-duct fairing on the longitudinal stability characteristics of the Langley free-flight-tunnel model with a  $35^\circ$  sweptback wing compared with UWAL tests of a larger model; vanes off; flaps  $0^\circ$ .

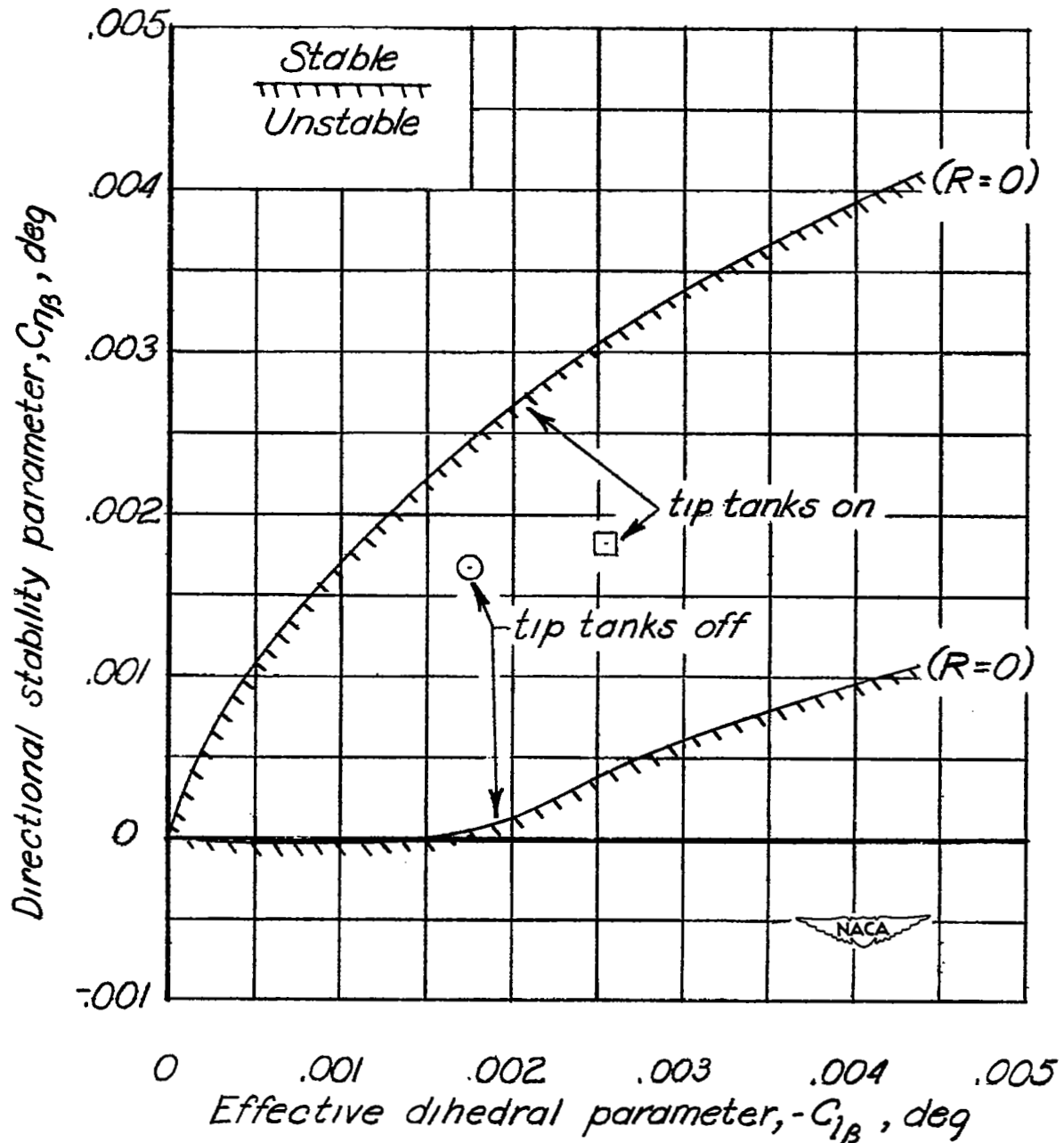
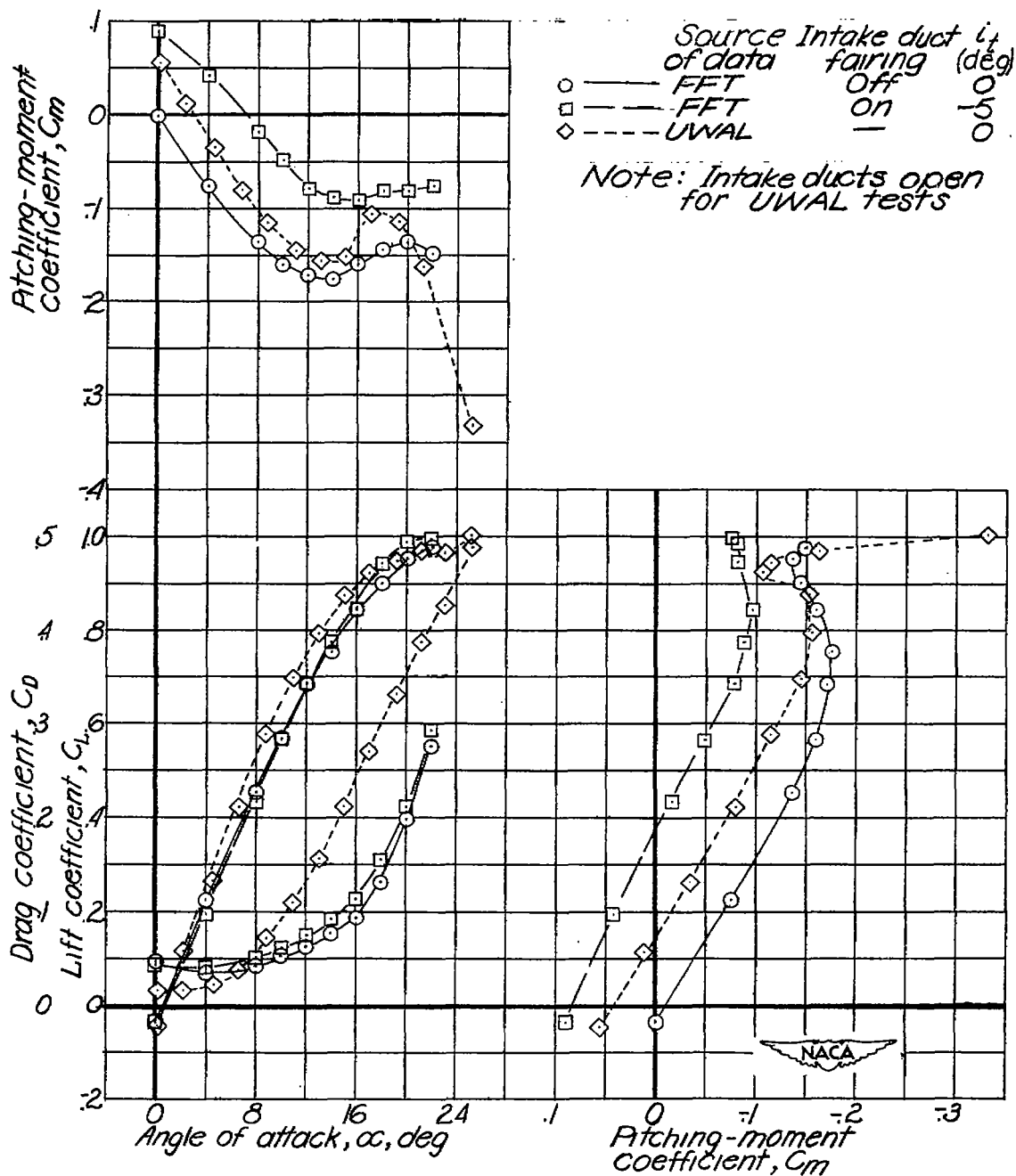
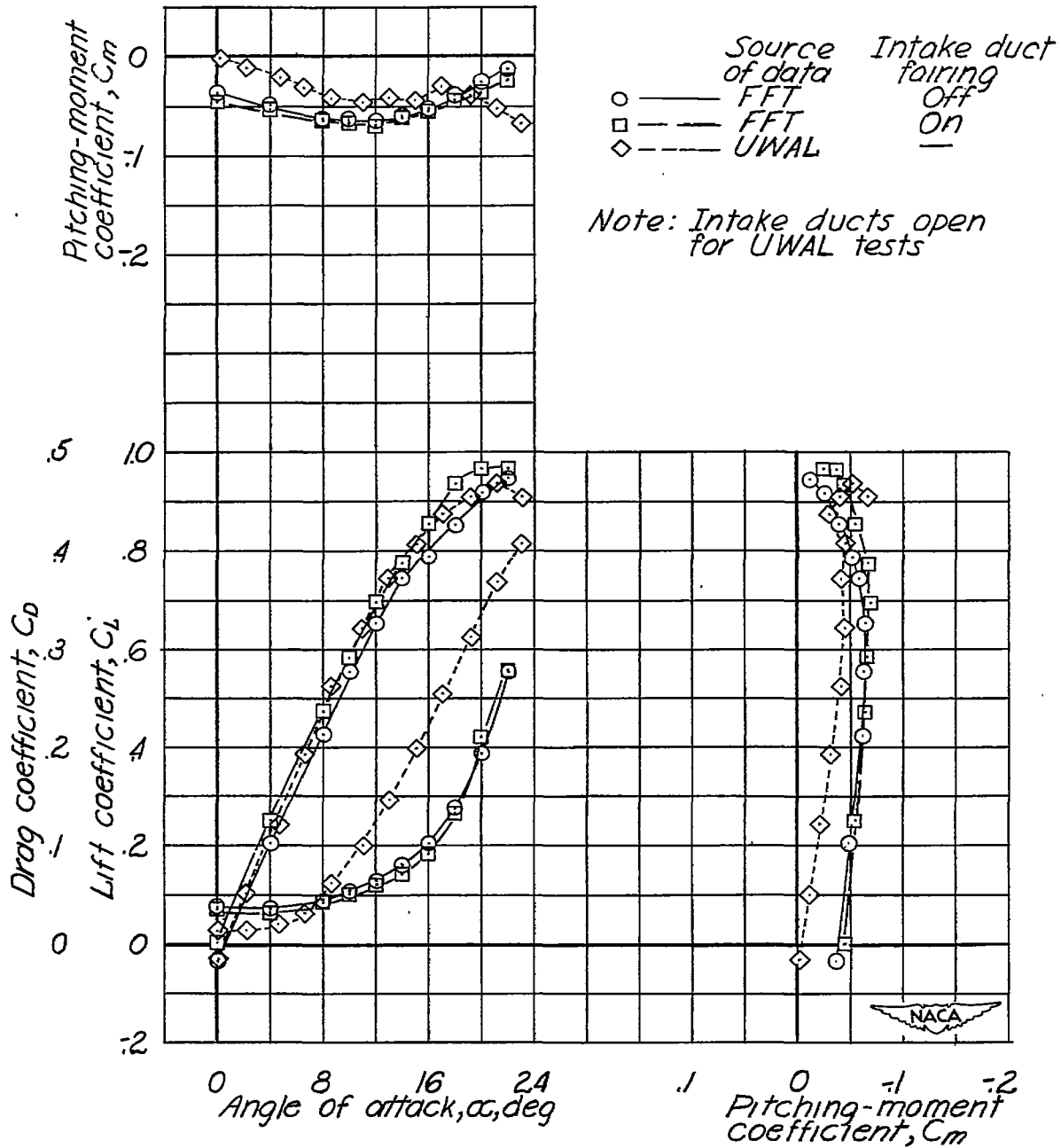


Figure 5.- Correlation of flight test points of a model with a 35° sweptback wing with calculated oscillatory stability boundaries;  $C_L = 0.7$ ;  $\delta_f = 0^\circ$ ; vanes and intake-duct fairings on.



(a) Tail on.

Figure 6.- Effect of intake-duct fairing on the longitudinal stability characteristics of the Langley free-flight-tunnel model with a  $35^\circ$  sweptback wing compared with UWAL tests of a larger model; vanes off; flaps  $0^\circ$ .



(b) Tail off.

Figure 6.- Concluded.

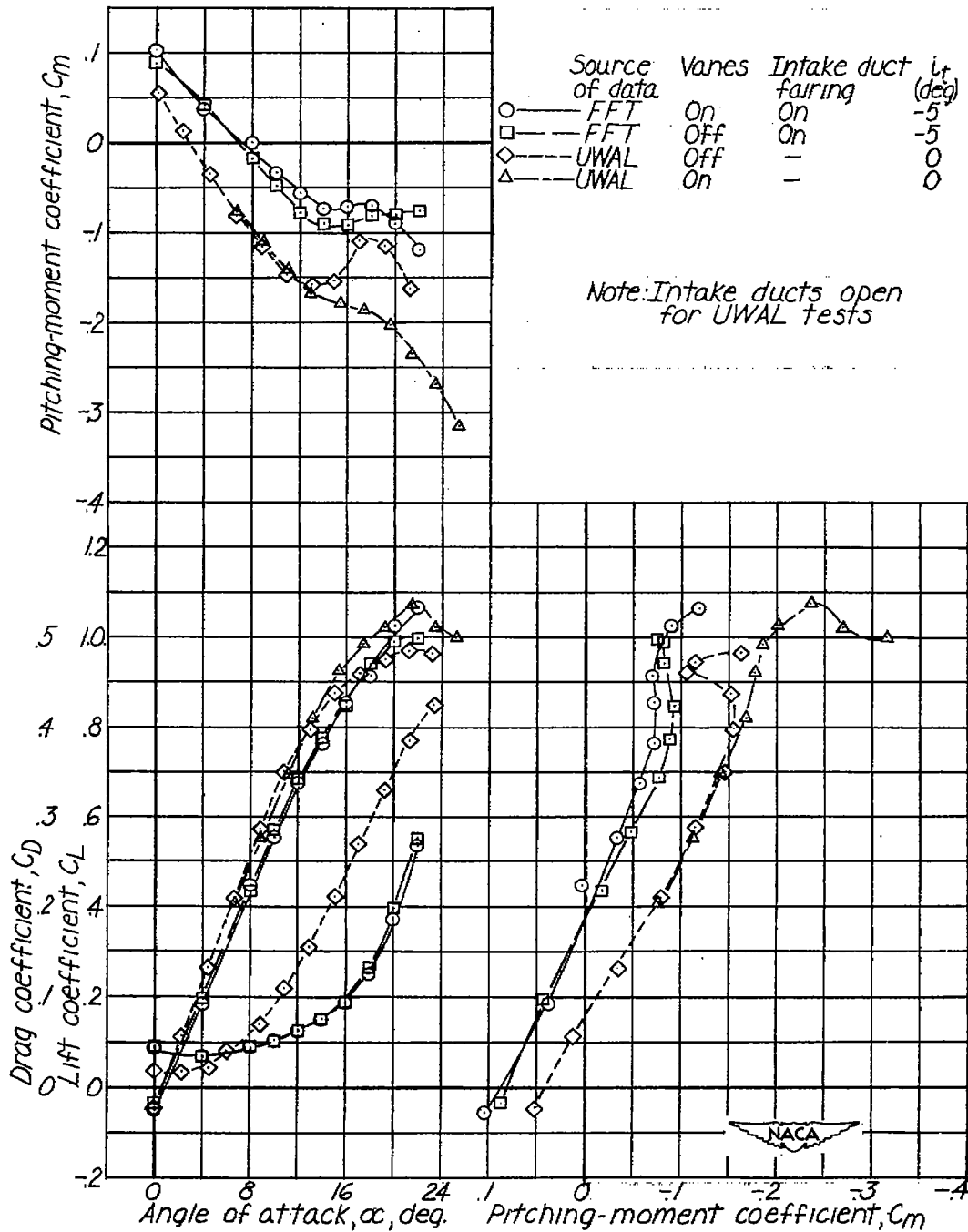


Figure 7.- The effect of stall-control vanes on the longitudinal stability characteristics of the Langley free-flight-tunnel model with a  $35^\circ$  sweptback wing compared with UWAL tests of a larger model; flaps  $0^\circ$ .

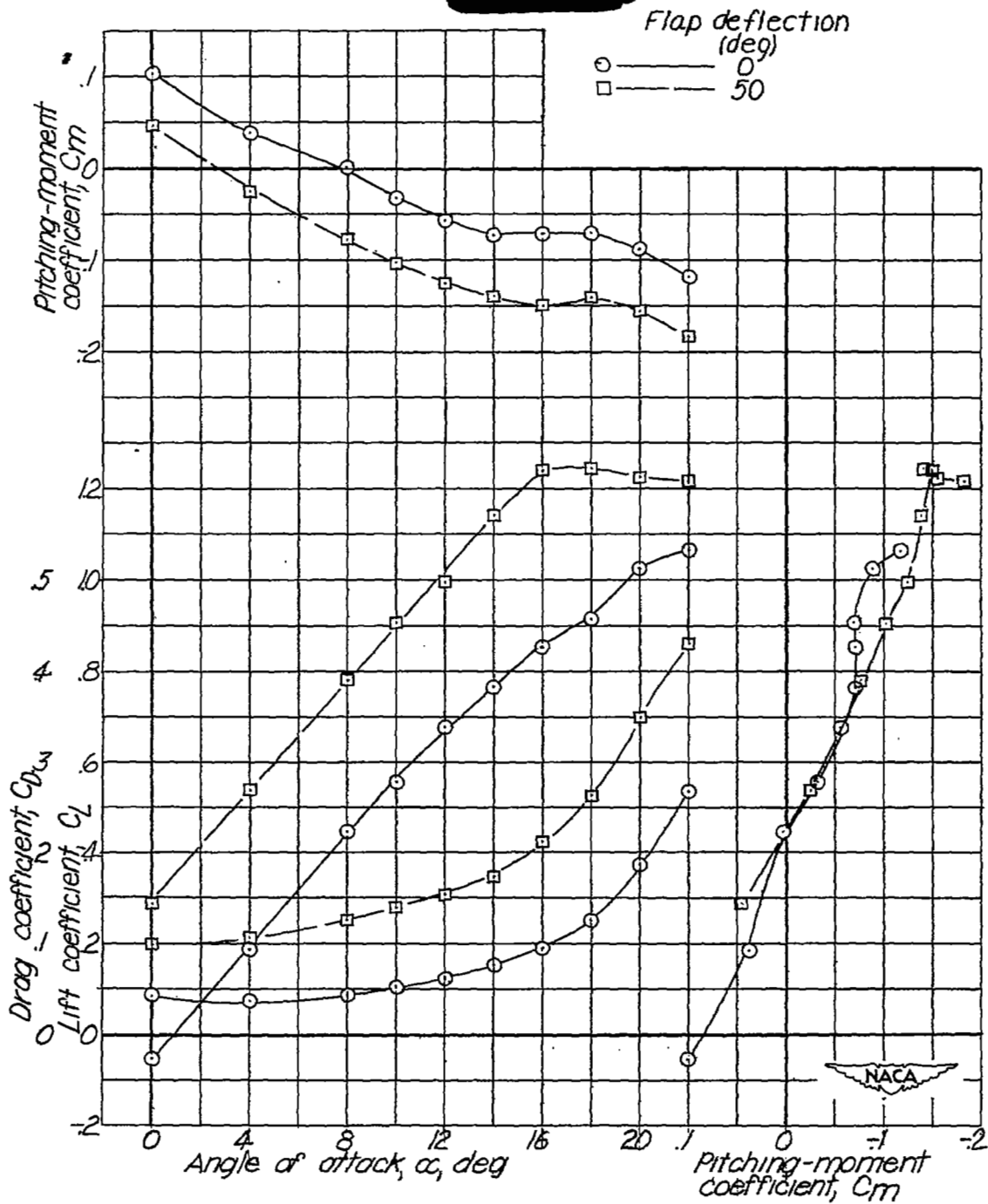


Figure 8.- The effect of flap deflection on the longitudinal stability characteristics of the Langley free-flight-tunnel model with a 35° sweptback wing; vanes and intake-duct fairings on;  $i_t = -5^\circ$ .

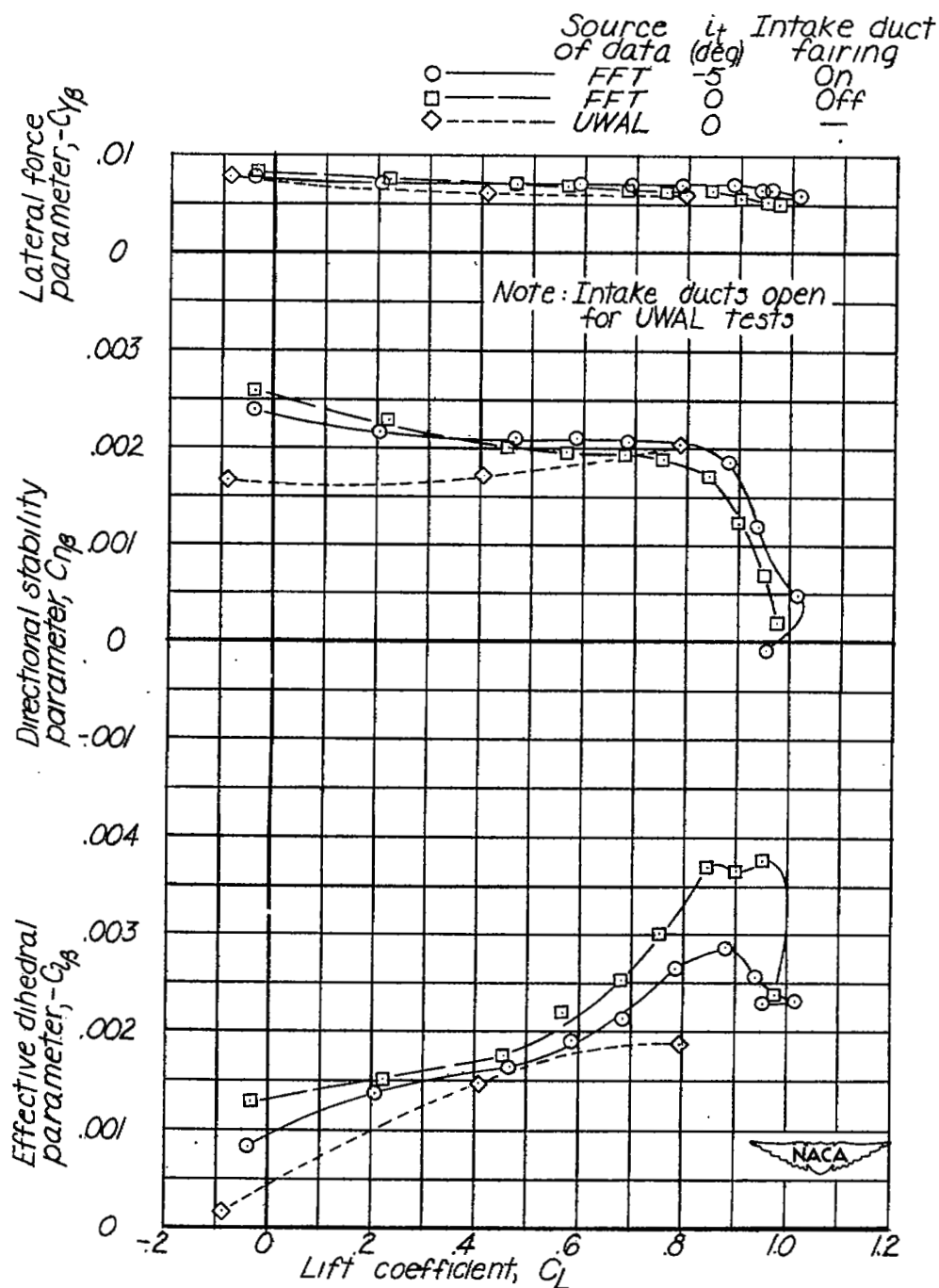


Figure 9.- The effect of duct fairing on the lateral stability characteristics of the Langley free-flight-tunnel model with a  $35^\circ$  sweptback wing compared with UWAL tests of a larger model; flaps  $0^\circ$ ; vanes off.

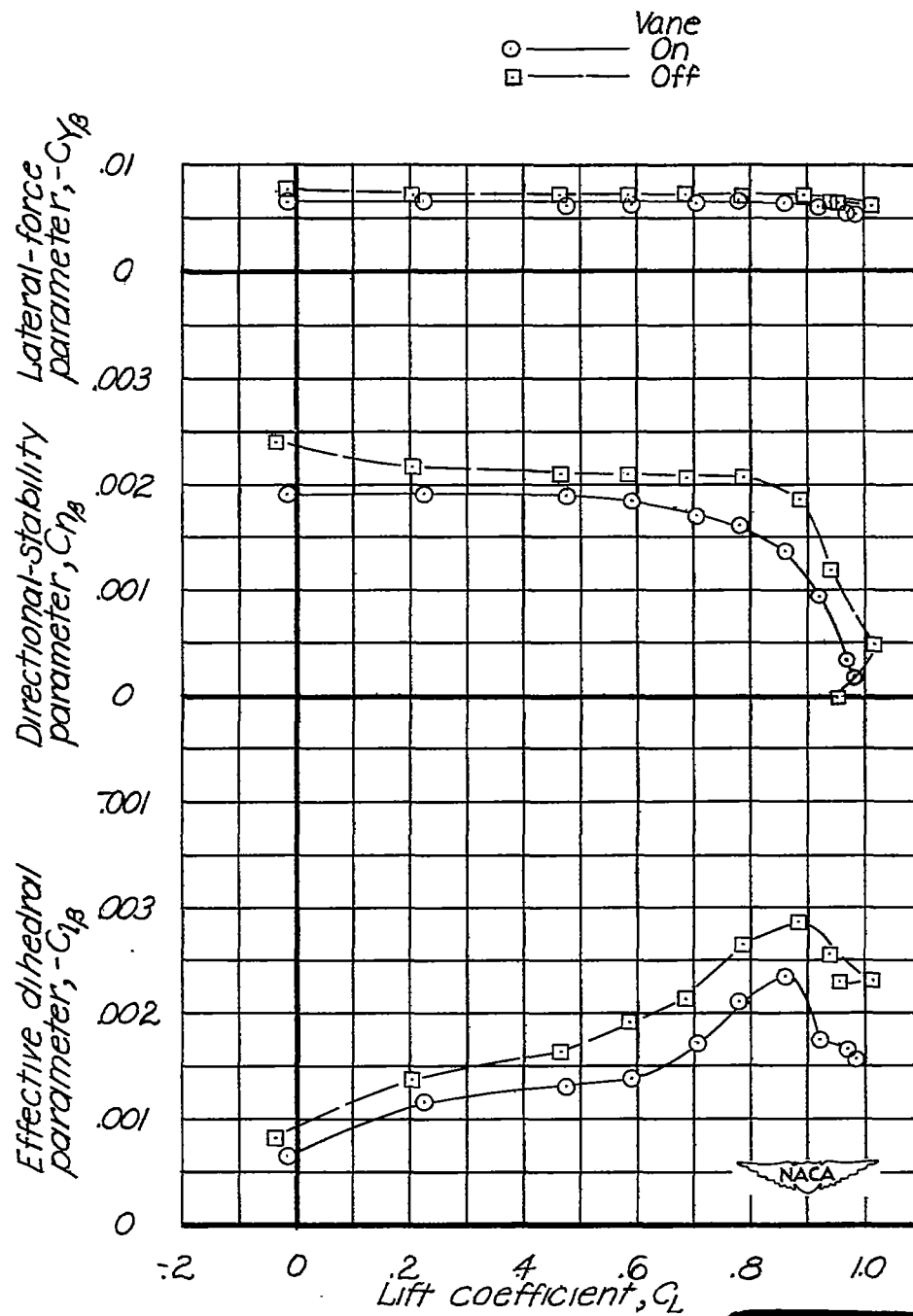


Figure 10.- The effect of the stall-control vanes on the lateral stability characteristics of the Langley free-flight-tunnel model with a 35° sweptback wing; flaps 0°; intake-duct fairing on;  $i_t = -5^\circ$ .

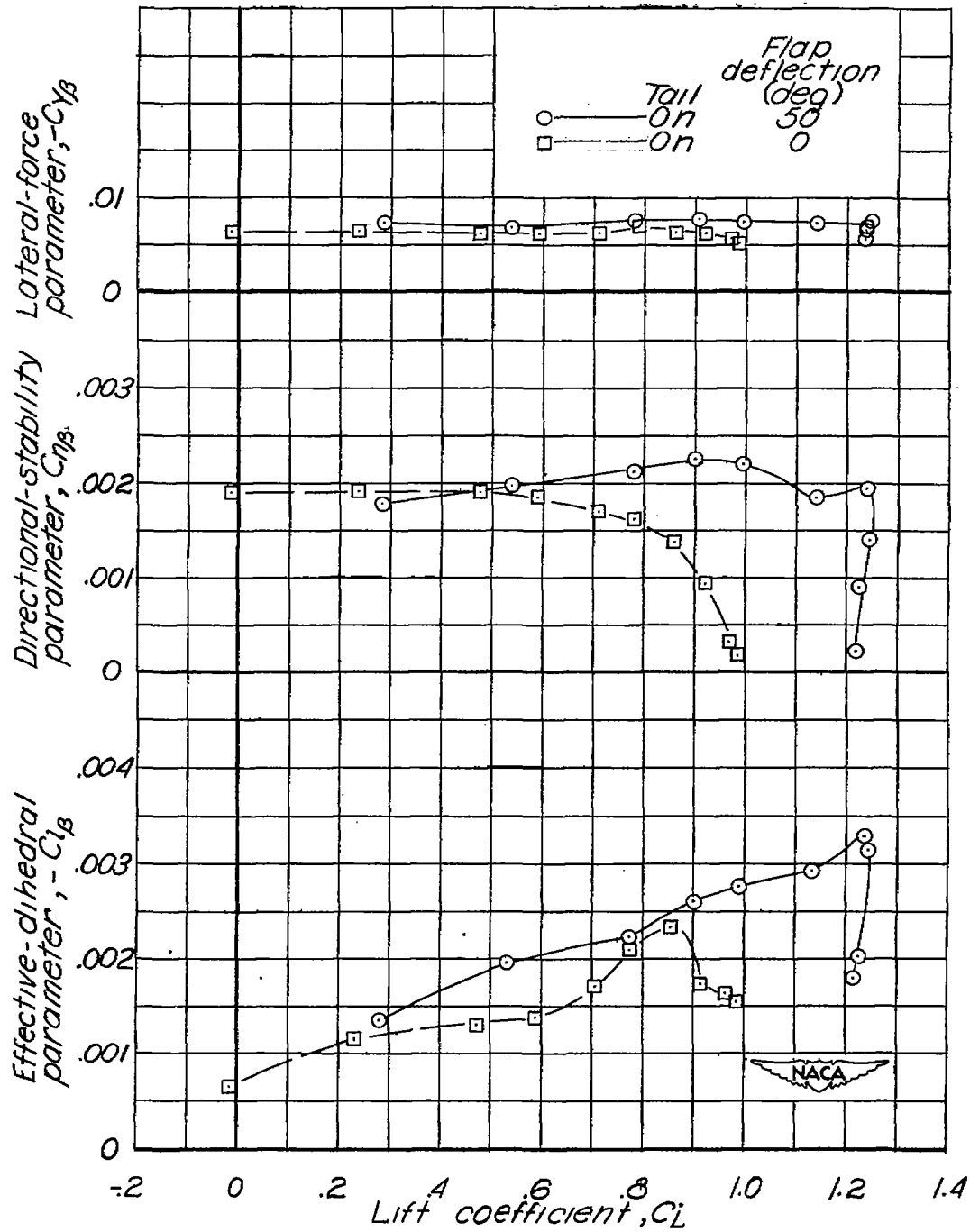


Figure 11.- The effect of flap deflection on the lateral stability characteristics of the Langley free-flight-tunnel model with a  $35^\circ$  sweptback wing; vanes and intake-duct fairings on;  $i_t = -5^\circ$ .

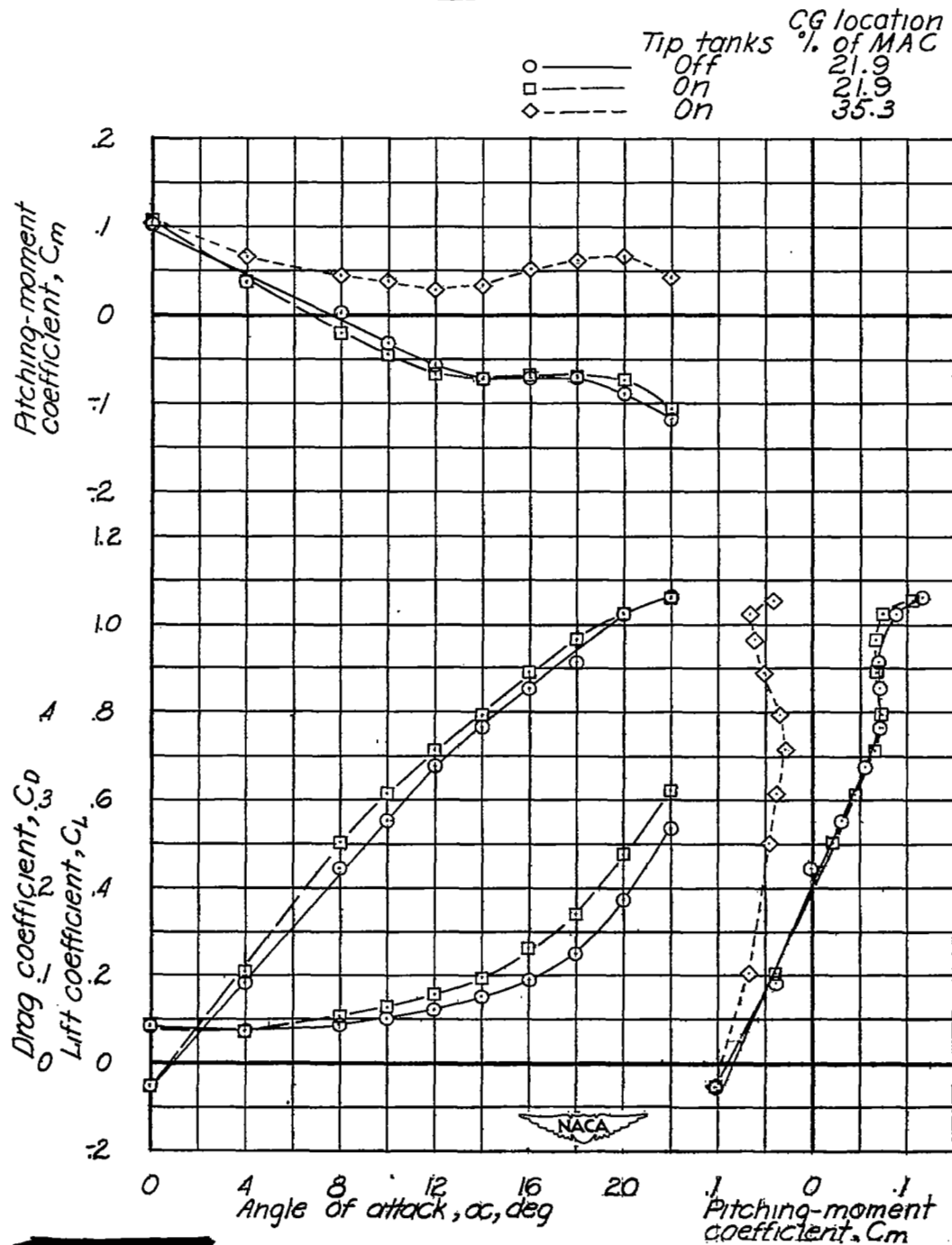


Figure 12.- The effect of wing-tip tanks and center-of-gravity positions on characteristics of the Langley free-flight-tunnel model with a 35° sweptback wing; vanes and intake-duct fairings on;  $i_t = -5^\circ$ .

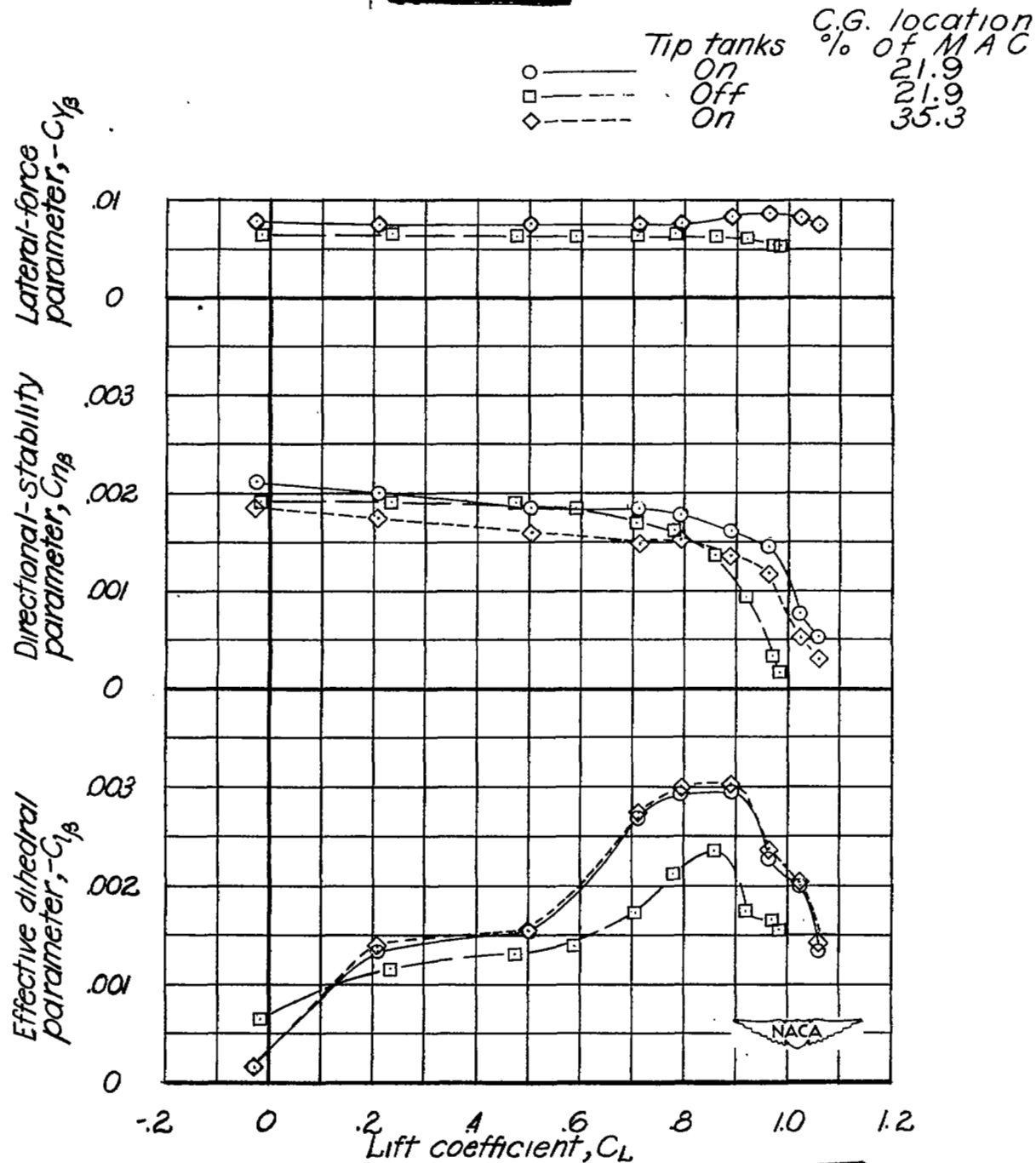
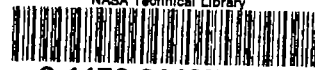


Figure 13.- The effect of wing-tip tanks and center-of-gravity positions on the lateral stability characteristics of the Langley free-flight-tunnel model with a  $35^\circ$  sweptback wing; vanes and intake-duct fairings on;  $i_t = -5^\circ$ .

NASA Technical Library



3 1176 01435 9443